Toxicology Reports 13 (2024) 101810

Contents lists available at ScienceDirect

Toxicology Reports

journal homepage: www.elsevier.com/locate/toxrep

Molecular docking and *in silico* analysis of the pharmacokinetics, toxicological profile and differential gene expression of bioactive compounds from *Cyrtopodium glutiniferum*

Natália Gonçalves Ribeiro Araujo [a,1], Francisco Carlos da Silva Junior [b,1], Lizandra Vitória de Souza Santos [a], Silvia Regina Batistuzzo de Medeiros [c], Israel Felzenszwalb [a], Carlos Fernando Araújo-Lima [a,d,*]

[a] *Laboratory of Environmental Mutagenesis, Department of Biophysics and Biometry, IBRAG/UERJ (University of the State of Rio de Janeiro), 87 - Fundos, 4th floor, Vila Isabel, Rio de Janeiro, RJ 20551-030, Brazil*

[b] *Toxicology Center, University of Saskatchewan, 44 Campus Dr, Saskatchewan S7N 5B3, Canada*

[c] *Laboratory of Biology and Molecular Mutagenesis, Department of Biology, Center for Biosciences/UFRN (Federal University of Rio Grande do Norte), 3000 Av. Sen. Salgado Filho-Lagoa Nova, Natal, RN 59064-741, Brazil*

[d] *Integrated Environmental Mutagenesis Laboratory, Federal University of Rio de Janeiro State (UNIRIO), R. Frei Caneca, 94 - Centro, Rio de Janeiro, RJ 20211-010, Brazil*

A R T I C L E I N F O

Handling Editor: Prof. L.H. Lash

Keywords:
Dihydroformononetin
Arbutin
Caffeic acid 4-O-glucoside
FADD
Caspases
Aurora kinases
HAT

A B S T R A C T

The genus *Cyrtopodium*, from the *Orchidaceae* family, is widely used for its therapeutic properties in the treatment of tuberculosis, abscesses, urinary infection, and colds. *C. glutiniferum*, one of the species of this genus, is endemic in Brazil and largely used in herbal medicine. Thus, it is of great interest to recognize its composition, the properties of the molecules found in it. This study aimed to perform the *in silico* analysis of the main compounds from *C. glutiniferum*, on the platforms pKCSM, SwissADME, LAZAR, CLC-pred, ToxTree, DIGEPred, STRING, and Cytoscape. Further than this, the molecular docking was performed. The compounds present in the aqueous extract of *C. glutiniferum* were identified by UHPLC-MS/MS, finding Arbutin, Caffeic acid 4-O-glucoside, and Dihydroformononetin as the three most abundant molecules. The evaluation of the gastrointestinal absorption of Dihydroformononetin is given as high, also managing to cross the blood-brain barrier, while Arbutin can only be absorbed by the gastrointestinal tract and Caffeic acid 4-O-glucoside had very low absorption. Further analysis showed that Arbutin and Dihydroformononetin are possible leading molecules for drug synthesis, according to the prediction. Toxicological aspects were analysed, and no adverse effects were noted, but there were divergences in the mutagenic prediction of Arbutin and Dihydroformononetin, having different results in the used platforms, demonstrating that a cautious analysis and data insertion is needed in these tools to optimize them. The analysis of the differentially expressed genes predicted that the compounds can regulate several genes, including some genes associated with carcinogenesis and inflammation. The Molecular docking analysis showed high binding affinities of the molecules with different proteins. Therefore, *C. glutiniferum* demonstrates the potential to be used as a phytotherapeutic. The same was given through the *in silico* analysis of the three compounds found in the orchid, that show good individual potential.

1. Introduction

Since the beginning of medicine, plants have been used due to their therapeutic activity. With the development of new technologies, there is a renewed interest in exploring the therapeutic potential of different plants and their molecules, looking for their safety, efficiency, and quality [1,2]. So, herbal medicine is an important source for the discovery of new molecules, since many plants metabolites databases have

* Corresponding author at: Integrated Environmental Mutagenesis Laboratory, Federal University of Rio de Janeiro State (UNIRIO), R. Frei Caneca, 94 - Centro, Rio de Janeiro, RJ 20211-010, Brazil.

E-mail addresses: biomed.carlos@gmail.com, araujo.lima@unirio.br (C.F. Araújo-Lima).

[1] These authors contributed equally in this study.

https://doi.org/10.1016/j.toxrep.2024.101810
Received 29 September 2024; Received in revised form 4 November 2024; Accepted 10 November 2024
Available online 15 November 2024

been originated within this analysis, making possible the synthesis of new complex molecules from the known ones, increasing the database of new compounds [3,4].

Orchids are a family that is largely used for their phytotherapeutic properties [5]. *Cyrtopodium glutiniferum* is an orchid from the genus *Cyrtopodium*. This genus is used in folk medicine for its gastroprotective and anti-inflammatory properties, in the treatment of urinary infections, burns, and colds, some of these aspects were observed in a couple of studies [6–9]. *Cyrtopodium glutiniferum* is frequently used in the treatment of abscesses, burns, tuberculosis, and boils, and as an anti-inflammatory. It was elucidated that this action happens because of the control of the inflammation promoted by this plant [10].

In our previous work, we identified the most abundant compounds in *Cyrtopodium glutiniferum*: Arbutin, Caffeic Acid 4-O-glucoside, and Dihydroformononetin [11]. The anti-inflammatory activity of the plant extract was observed using *in vitro* models. Exploring and analysing the potential of these prevalent molecules for new drug development is particularly intriguing due to their recognizability. The *in silico* approach, utilizing structure–activity relationships (SARs) and quantitative structure–activity relationships (QSARs), is crucial in the drug discovery process [12]. These models enable the virtual screening of potential new drugs by predicting their physicochemical, biological, and environmental properties, thereby reducing the need for animal testing in toxicology studies [13,14].

These compounds showed notable potential in previous studies, both *in vitro* and *in vivo* activities. Arbutin is already used in the skin beauty field and exhibited anticancer and anti-inflammatory activity, and potential in the treatment of diabetes, osteoporosis, and CNS disorders [15–17]. The Caffeic Acid 4-O-glucoside showed effectivity in the axonal regeneration *in vivo*, this might be helpful in memory deficits associated with Alzheimer's disease [18]. Dihydroformononetin is a reduced metabolite of Formononetin [19], and this last molecule shows several therapeutic properties such as hepatoprotection, good perspective in the treatment and prevention of obesity, cancer, atherosclerosis, and neurodegenerative diseases [20–23]. However, their ADMET properties, toxicity, and molecular interactions have been poorly explored, with most studies focusing primarily on Arbutin [24,25].

Observing the potential of the compounds found in this orchid and knowing the relevance of *in silico* approaches for drug discovery, it is important to analyse whether these molecules are good candidates for new drugs or how they modulate the gene expression, concomitant, their safety. Thus, this research aims perform in silico analysis and molecular docking of the main compounds from *Cyrtopodium glutiniferum* to evaluate their pharmacokinetic properties, toxicity, molecular interactions, and potential for gene regulation, thereby assessing their suitability for drug development.

2. Materials and methods

2.1. Pharmacokinetic analysis

The pharmacological properties of Dihydroformononetin, Arbutin, and Caffeic acid 4-O-glucoside were analysed through the *in silico* algorithms pkCSM and SwissADME. Their canonical SMILES sequence was obtained in PubChem (https://pubchem.ncbi.nlm.nih.gov/) [26] and used as input in each platform. The pkCSM (http://biosig.unimelb.edu.au/pkcsm/prediction) makes its predictions based on the molecule graph-based signatures and gives data about the pharmacokinetic and toxicological characteristics of the molecules [27]. Swiss ADME (http://www.swissadme.ch/) predicts pharmacokinetic properties and interesting aspects of a new drug. For its prediction, this algorithm uses a method results in-house, directly calculated from non-commercial executables or implemented from publications [28].

2.2. Toxicological analysis

The toxicologic analysis was performed with the algorithm LAZAR, which is based on QSAR (quantitative structure-activity relationship) to make its predictions [29]. Some toxicological results were also obtained in the previous pkCSM analysis, as mentioned before. The cytotoxicity prediction was performed in CLC-pred (http://www.way2drug.com/cell-line/), an analysis based on the Prediction of Activity Spectra for Substances (PASS) [30]. ToxTree software was used for a few toxicological parameters [31]. To perform the predictions, these decision trees were selected: "*in vitro* mutagenicity (AMES test)", "structural alerts for the *in vivo* micronucleus assay in rodents" and "carcinogenicity". So the software is able to provide different decision trees to estimate the toxic effect [32,33]. For all of them, the input was the same, the Canonical SMILES sequence obtained in PubChem.

2.3. Differentially expressed gene (DEG) analysis

For the analysis of the effect on the gene expression of each molecule, DIGEP-Pred was used to perform each prediction. The results were inserted in the STRING database (version 11.5) and organized according to their protein-protein interaction (PPI), after, on Cytoscape. On DIGEP-pred, the Canonical SMILES sequence was the input for the prediction of genes that were up or downregulated [34]. The data obtained was the new input for STRING (https://string-db.org/) [35], where it was possible to enrich the gene network connection via automated text mining and previous knowledge in databases, the confidence score was high (0.700). The obtained network was inserted at Cytoscape [36] and used with the plugin Cytohubba [37] for the prediction of the centrality measures Degree and Betweenness. The Degree measures how many direct connections a node has, the ones that are highly connected are called "hubs" of a PPI network and they play a fundamental role in the exchange of information [38]. The Betweenness centrality evaluates the extent of the shortest paths between vertices that, in the network, pass through a node, therefore, a node with high betweenness connects subnets of a network, being essential for the propagation of information they are called "bottlenecks" [39]. The nodes with high degree and high betweenness are called "hub-bottleneck" (N-HB) and can play an elementary role in the regulation of biological processes, deregulation in them may lead to network fragmentation, which makes important the analysis of transcriptional expression when affected by different compounds.

2.4. Ligand and receptor preparation

The 3D structure of the Arbutin, Caffeic acid, and Dihydroformononetin were downloaded from PubChem database (https://pubchem.ncbi.nlm.nih.gov/) in SDF format. The structures were further converted into PDBQT format using Open Babel Software (version 2.3.1). MMFF94 force field and conjugate gradient optimization algorithm were used to minimize the ligand energy in 200 steps using PyRx-Python prescription 0.8.

The 3D crystal structure of the N-NBs was retrieved from RCSB protein data bank (https://www.rcsb. org/). The resolution of the obtained structures was approximately 1.18 Å. The file was opened using the Discovery Studio Visualizer (DSV) Client Program (v17.2.0.16349). Water molecules were removed with AutoDock tools, and subsequently, polar hydrogen atoms, Gasteiger partial charges, and Kollman charges were added to the targets. Thereafter, the protein was then saved in pdb format.

2.5. Molecular docking

The original ligand was re-docked on the target receptor to validate the docking method. The DSV was used to remove this ligand from the receptor. The grid box parametric dimension values were provided in

the Supplementary material 2 and were used as coordinate centers. The exhaustiveness value was set as 8 to obtain an efficient binding conformation pose of the protein–ligand complex. Afterward, the retrieved phytochemicals were docked against their respective N-HBs. Auto Dock Vina was used to perform dock simulation. Auto Dock Vina generated a docked complex for each ligand and respective N-HBs with different conformation and affinity scores (in kcal/mol) and ordered according to the lowest binding energy theory (kcal/mol) of docked complexes, thus, more negative values mean higher binding affinity. Thereafter, the DSV was used to analyse and graphically visualize the best protein-ligand complex docked pose.

3. Results

Dihydroformononetin can permeate the Blood-Barrier Brain (BBB) and be well absorbed by the Gastrointestinal Tract (GIT) (Fig. 1). Still, according to the predictions, Arbutin can be absorbed by GIT but cannot permeate thee BBB. Caffeic acid 4-O-glucoside showed neither of these properties. Some desirable characteristics for a drug like liposolubility, size, polarity, insolubility, unsaturation, and flexibility were predicted in the Radar Graphic (Fig. 2), the Caffeic acid 4-O-glucoside polarity was bigger than the desirable, like the unsaturation number of Dihydroformononetin.

Different pharmacokinetic properties (ADME) were predicted in two algorithms: pKCSM and SwissADME. The water solubility of Arbutin was 0.86 mmol/L according to pKCSM and 2.083 in SwissADME. The gastrointestinal absorption (GI) prediction in pKCSM was 38.02 %, while for SwissADME it was predicted as highly absorbed. The skin permeability was −2.087 log Kp and −8.98 log Kp in pKCSM and SwissADME, respectively. Arbutin was not predicted as a substrate or inhibitor of P-glycoprotein. The pKCSM predicted the volume of distribution (VDss) as 1.07 L/kg, the fraction unbound as 0.784 Fu, and the Central Nervous System (CNS) permeability as −3.557 log PS. The BBB permeability prediction was −0.962 log BB in pKCSM and for SwissADME the molecule cannot premeate the BBB. The molecule did not show any interactions with the predicted CYPs. The total clearance was 3341 log mL/min/kg and did not show interaction with renal OCT2 substrate according to pKCSM (Table 1).

The water solubility of Caffeic acid 4-O-glucoside was predicted as 4.456 mmol/L in pKCSM and 2.862 mol/L in SwissADME. The GI absorption was 14.025 % in pKCSM and Low by SwissADME. The skin permeability was predicted as −2.735 log Kp and −9.06 log Kp in pKCSM and SwissADME, respectively. The molecule did not show interaction with P-glycoprotein. The VDss prediction was 0.171 L/kg, the fraction unbound of 0.654 Fu, and the CNS permeability of −4.103 log PS according to pKCSM. The BBB permeability prediction in pKCSM was −1.261 log BB and for SwissADME the molecule cannot permeate the BBB. Like Arbutin, Caffeic acid 4-O-glucoside did not show any interactions with the predicted CYPs. The prediction in pKCSM of the total clearance was 0.134 log mL/min/kg and did not show interaction with renal OCT2 substrate (Table 2).

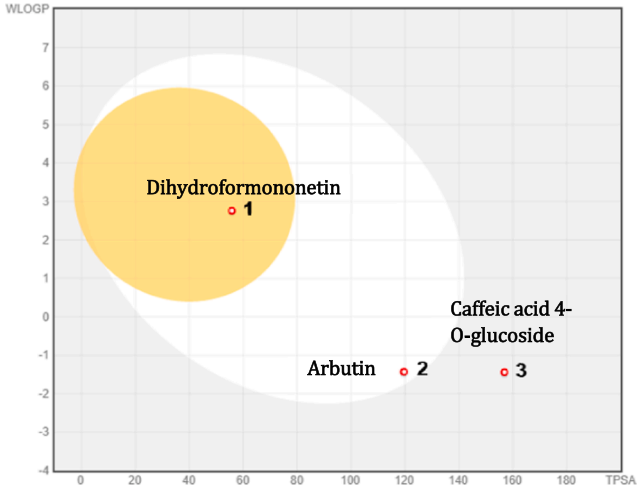

Fig. 1. SwissADME Boiled-egg graphic with the three analysed compounds. The yellow area indicates the substances that are capable of permeate the BBB, like Dihydroformononetin. The white area indicates the compounds that can be absorbed by the GIT, like Arbutin and Dihydroformononetin. Caffeic acid 4-O-glucoside did not show any of these properties. All the substances are in red dots, which means that they are not substrates for glycoprotein P.

The ADME properties of Dihydroformononetin were predicted too. The water solubility according to pKCSM was 0.3 mmol/L and 0.266 in SwissADME. The GI absorption was 95.51 % in pKCSM and predicted as high absorbed in SwissADME. The skin permeability was −2.817 log Kp and −6,04 log Kp in pKCSM and SwissADME, respectively. Like the other molecules, Dihydroformononetin was not predicted as a substrate or inhibitor of P-glycoprotein. The prediction of the VDss was 1.044 L/kg, the fraction unbound was 0.058 Fu, and the CNS permeability of −2.131 log PS, according to pKCSM. The BBB permeability was 0.207 log BB in pKCSM prediction and SwissADME predicted that Dihydroformononetin can permeate BBB, differently from the other molecules. The prediction of the interaction with different CYPs showed that Dihydroformononetin can be a substrate of CYP3A4 and inhibit CYP1A2, CYP2C19, CYP2C9, and CYP3A4. The total clearance was 1.25 log mL/min/kg and did not show interaction with renal OCT2 substrate according to pKCSM (Table 3).

Toxicological aspects were predicted by pKCSM and LAZAR (Table 4). The Ames toxicity had divergent results in the predictions of Arbutin and Dihydroformononetin, while Caffeic acid 4-O-glucoside was predicted as non-mutagenic. Arbutin was not predicted as an hERG inhibitor, hepatotoxic, or skin sensitizer in pKCSM. The LD50 of Arbutin was 1.641 mol/kg, of Caffeic acid 4-O-glucoside was 2.342 mol/kg and of Dihydroformononetin was 2.579 mol/kg, according to pKCSM prediction. Arbutin LOAEL prediction was 3140 mg/kg/day in pKCSM and 871 mg/kg/day in LAZAR. Dihydroformononetin's LOAEL was 103.5 mg/kg/day in pKCSM and 102 mg/kg/day in LAZAR. Caffeic acid 4-O-glucoside LOAEL was 11.428 mg/kg/day in pKCSM prediction. The Arbutin maximum tolerated dose for humans was 3.07 mg/kg/day in pKCSM and 33.7 mg/kg/day in LAZAR. For Caffeic acid 4-O-glucoside, it was predicted as 3.273 mg/kg/day in pKCSM and 15.1 mg/kg/day in LAZAR. Dihydroformononetin's maximum tolerated dose for humans was 1.67 mg/kg/day in pKCSM and 6.67 mg/kg/day in LAZAR. None of them was predicted as carcinogenic in rodents by pKCSM.

According to ToxTree prediction, none of them showed carcinogenicity too (Table 5).

The three molecules showed at least one structural alert for micronucleus. None of them showed alerts for inducing mutagenicity by the Ames test in this predictor.

The CLC-pred predicted that Arbutin can be cytotoxic for 111 tumoral cell lines and 9 non-tumoral. Caffeic acid 4-O-glucoside was predicted as cytotoxic for 77 tumoral cell lines and 6 non-tumoral, while Dihydroformononetin was cytotoxic to 51 tumoral cell lines and 10 non-tumoral according to CLC-pred prediction (Table 6).

The prediction of drug inducing changes in gene expression profiles was also performed. According to this, each molecule was capable of regulating the expression of many genes. First, the gene network was formed using STRING (results not shown), showing the connections between the genes that were regulated by the three molecules and their connections with others. Genes that played significant roles in modulating the gene network were identified by their Degree and Betweenness, as the value increases, the color becomes progressively redder. Conversely, as the value decreases, the color shifts towards yellow. The gene names are describes in Supplementary Material 1 and the values of the hub-bottlenecks are available in the Supplementary Material 3. The predicted genes upregulated by Arbutin were NOTCH1, RBPJ, HIF1A, EP300, CTNNB1, HES1, HSP90AA1 and SRC (Fig. 3). The upregulated

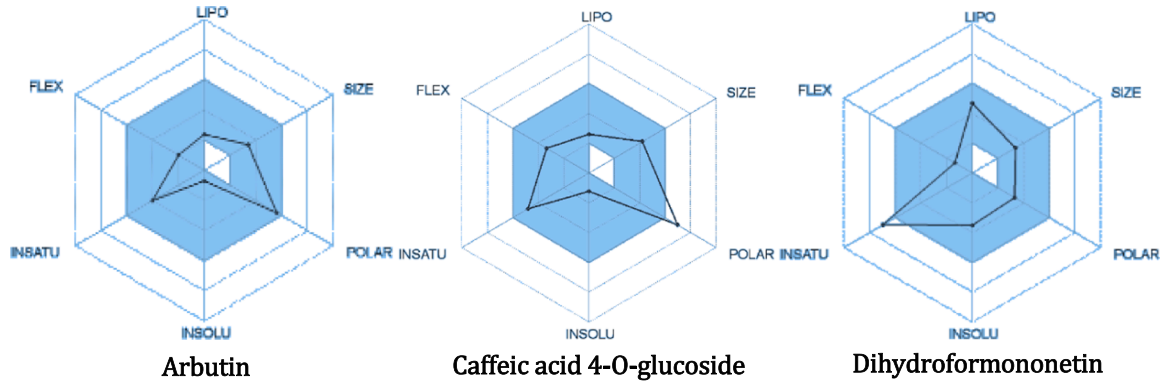

Fig. 2. SwissADME radar graphic of each molecule analysed. The desirable characteristics of a drug are inside the blue part of the graphic. LIPO = liposolubility, size, POLAR = polarity, INSOLU = insolubility, INSATU = unsaturation and FLEX = flexibility.

Table 1
Comparison between pKCSM and SwissADME pharmacokinetic (ADME) properties prediction of Arbutin.

	pKCSM		SwissADME	
Model name	Unit	Prediction	Unit	Prediction
Water solubility (consensus)	Numeric (mmol/L)	0.86	Numeric (mol/L)	2.083
GI absorption (human)	Numeric (% Absorbed)	38.02	Categorical (Low/High)	High
Skin Permeability	Numeric (log Kp)	−2.087	Numeric (log Kp)	−8.92
P-glycoprotein substrate	Categorical (Yes/No)	No	Categorical (Yes/No)	No
P-glycoprotein inhibitor	Categorical (Yes/No)	No	n.a.	—
VDss (human)	Numeric (L/kg)	1.07	n.a.	—
Fraction unbound (human)	Numeric (Fu)	0.784	n.a.	—
BBB permeability	Numeric (log BB)	−0.962	Categorical (Yes/No)	No
CNS permeability	Numeric (log PS)	−3.557	n.a.	—
CYP2D6 substrate	Categorical (Yes/No)	No	n.a.	—
CYP3A4 substrate	Categorical (Yes/No)	No	n.a.	—
CYP1A2 inhibitor	Categorical (Yes/No)	No	Categorical (Yes/No)	No
CYP2C19 inhibitor	Categorical (Yes/No)	No	Categorical (Yes/No)	No
CYP2C9 inhibitor	Categorical (Yes/No)	No	Categorical (Yes/No)	No
CYP2D6 inhibitor	Categorical (Yes/No)	No	Categorical (Yes/No)	No
CYP3A4 inhibitor	Categorical (Yes/No)	No	Categorical (Yes/No)	No
Total Clearance	Numeric (log mL/min/kg)	3341	n.a.	—
Renal OCT2 substrate	Categorical (Yes/No)	No	n.a.	—

GI: gastrointestinal; VDss: volume of distribution at steady state; BBB: brain blood barrier; CNS: central nervous system; CYP: cytochrome P; OCT: organic cation transporter; n.a.: not analysed.

Table 2
Comparison between pKCSM and SwissADME pharmacokinetic (ADME) properties prediction of Caffeic acid 4-O-glucoside.

	pKCSM		SwissADME	
Model name	Unit	Prediction	Unit	Prediction
Water solubility (consensus)	Numeric (mmol/L)	4.456	Numeric (mol/L)	2.862
GI absorption (human)	Numeric (% Absorbed)	14.025	Categorical (Low/High)	Low
Skin Permeability	Numeric (log Kp)	−2.735	Numeric (log Kp)	−9.06
P-glycoprotein substrate	Categorical (Yes/No)	No	Categorical (Yes/No)	No
P-glycoprotein inhibitor	Categorical (Yes/No)	No	n.a.	—
VDss (human)	Numeric (L/kg)	0.171	n.a.	—
Fraction unbound (human)	Numeric (Fu)	0.654	n.a.	—
BBB permeability	Numeric (log BB)	−1.261	Categorical (Yes/No)	No
CNS permeability	Numeric (log PS)	−4.103	n.a.	—
CYP2D6 substrate	Categorical (Yes/No)	No	n.a.	—
CYP3A4 substrate	Categorical (Yes/No)	No	n.a.	—
CYP1A2 inhibitor	Categorical (Yes/No)	No	Categorical (Yes/No)	No
CYP2C19 inhibitor	Categorical (Yes/No)	No	Categorical (Yes/No)	No
CYP2C9 inhibitor	Categorical (Yes/No)	No	Categorical (Yes/No)	No
CYP2D6 inhibitor	Categorical (Yes/No)	No	Categorical (Yes/No)	No
CYP3A4 inhibitor	Categorical (Yes/No)	No	Categorical (Yes/No)	No
Total Clearance	Numeric (log mL/min/kg)	0.134	n.a.	—
Renal OCT2 substrate	Categorical (Yes/No)	No	n.a.	—

GI: gastrointestinal; VDss: volume of distribution at steady state; BBB: brain blood barrier; CNS: central nervous system; CYP: cytochrome P; OCT: organic cation transporter; n.a.: not analysed.

by Caffeic acid 4-O-glucoside were: HIF1A, ITGB1, RBPJ, EP300, NOTCH1, PSEN1, ITGA3, CREBBP, CTNNB1 and ITGA5 (Fig. 4). The ones upregulated by Dihydroformononetin were: CDC20, GMNN, CDC6, AURKB, and AURKA (Fig. 5).

The downregulation of gene expression was evaluated as well. The main genes predicted to be downregulated by Arbutin were: SKP1, DBB1, RBX1, GSK3B, NEDD8, APC, AXIN1, and PSMD3 (Fig. 6). The downregulated by Caffeic acid 4-O-glucoside were RBX1, AXIN1, APC, SKP1, NEDD8, HSP90AA1, PSMD3 and HDAC1 (Fig. 7). The downregulated by Dihydroformononetin were CASP8, FADD, and EXOC8 (Fig. 8).

The molecular docking analysis was performed for the three molecules, Arbutin, Caffeic acid 4-O-glucoside and Dihydroformononetin, and the proteins of the found hub-bottlenecks that would be affected by the DIGEP. The results are expressed on Tables 7, 8 and 9. It is possible to notice that the binding energy of some of the complex protein-ligands

Table 3
Comparison between pKCSM and SwissADME pharmacokinetic (ADME) properties prediction of Dihydroformononetin.

	pKCSM		SwissADME	
Model name	Unit	Prediction	Unit	Prediction
Water solubility (consensus)	Numeric (mmol/L)	0.3	Numeric (mol/L)	0.266
GI absorption (human)	Numeric (% Absorbed)	95.51	Categorical (Low/High)	High
Skin Permeability	Numeric (log Kp)	−2.817	Numeric (log Kp)	−6.04
P-glycoprotein substrate	Categorical (Yes/No)	No	Categorical (Yes/No)	No
P-glycoprotein inhibitor	Categorical (Yes/No)	No	n.a.	—
VDss (human)	Numeric (L/kg)	1.044	n.a.	—
Fraction unbound (human)	Numeric (Fu)	0.058	n.a.	—
BBB permeability	Numeric (log BB)	0.207	Categorical (Yes/No)	Yes
CNS permeability	Numeric (log PS)	−2.131	n.a.	—
CYP2D6 substrate	Categorical (Yes/No)	No	n.a.	—
CYP3A4 substrate	Categorical (Yes/No)	Yes	n.a.	—
CYP1A2 inhibitor	Categorical (Yes/No)	Yes	Categorical (Yes/No)	Yes
CYP2C19 inhibitor	Categorical (Yes/No)	Yes	Categorical (Yes/No)	Yes
CYP2C9 inhibitor	Categorical (Yes/No)	Yes	Categorical (Yes/No)	Yes
CYP2D6 inhibitor	Categorical (Yes/No)	No	Categorical (Yes/No)	No
CYP3A4 inhibitor	Categorical (Yes/No)	Yes	Categorical (Yes/No)	Yes
Total Clearance	Numeric (log mL/min/kg)	1.25	n.a.	—
Renal OCT2 substrate	Categorical (Yes/No)	No	n.a.	—

GI: gastrointestinal; VDss: volume of distribution at steady state; BBB: brain blood barrier; CNS: central nervous system; CYP: cytochrome P; OCT: organic cation transporter; n.a.: not analysed.

are low, revealing a high binding affinity. The interactions with lower binding energy are displayed on Figs. 9, 10 and 11. All the lowest binding energies are displayed in red, according to its expression status.

The lowest binding energy of Arbutin is with CTNNB1 at −7.5 kcal/mol. Among those with downregulation status, DDB1 has the lowest binding energy at −7.0 kcal/mol. For Caffeic acid 4-O-glucoside, the lowest binding energy is with ITGA3 at −8.1 kcal/mol, and among the downregulated, APC shows the lowest at −6.8 kcal/mol. Dihydroformononetin has the lowest binding energy with AURKB at −8.9 kcal/mol, while CASP8 and EXOC8 have the lowest binding energies among the downregulated targets, both at −6.8 kcal/mol.

4. Discussion

Many molecules are being studied for their therapeutic potential. A lot of them have origin in natural products, with notorious relevance for drug discovery. Given the vast array of new molecules, prioritizing those with significant potential to evolve into new medicines is crucial. Therefore, bioinformatics has become an important tool in the screening of these molecules before the *in vitro* and *in vivo* analysis [4]. Many parameters were analysed evaluating the pharmacokinetics, toxicology, interference in gene expression and molecular docking of the three molecules.

The pharmacokinetic analyses showed that Arbutin and Dihydroformononetin may be well absorbed by the GIT, but Caffeic acid 4-O-glucoside cannot, as shown in the Boiled-egg graphic and the pharmacokinetic properties table. The prediction showed also that only Dihydroformononetin can permeate the BBB. This is an important aspect that can be well used with caution since this molecule can interact with the Central Nervous System and leads to unintended effects [40]. The radar graphic prediction showed that most of the properties, like insaturation, insolubility, polarity, molecule size, liposolubility and flexibility were in the criteria for a potential new drug, except for Cafeic acid 4-O-glucoside polarity and Dihydroformononetin insaturation.

None of the molecules serves as an inhibitor or substrate for P-glycoprotein, a protein that functions in protecting against xenobiotics by facilitating their efflux from cells, thereby diminishing their bioavailability. [41]. The metabolism aspects exhibited that Arbutin and Caffeic Acis 4-O-glucoside did not interact with the family of enzymes from Cytochrome P450, but Dihydroformononetin shows different interactions with them, as an inhibitor and as a substrate of these enzymes. It is important to consider the generation of metabolites, how they will interact with the organism, and the consequences of the inhibition of the activity of some enzymes, since the metabolism of other molecules may not happen for this reason [42]. An example of the modulation that some molecules can cause in the functionality of the P450 enzyme is described by Jacobson [43], in which simvastatin and atorvastatin had different drug interaction profiles when co-administered with Cytochrome P450 inhibitors, what did not happen with pravastatin.

The prediction of mutagenicity (Ames Test) showed divergent results for Arbutin and Dihydroformononetin, and ToxTree's prediction indicated that all three molecules possessed at least one structural alert for inducing micronuclei. In previous studies conducted *in vitro*, the *Cyrtopodium glutiniferum* aqueous extract only showed mutagenic activity in the higher concentration, 5000 μg/plate, and only in the TA100 strain with metabolic activation among five strains analysed with and without S9. The *in vitro* Micronucleus assay was performed and none of the tested concentrations induced micronuclei [11].

These findings indicate the potential limitations in the current *in silico* platforms. The *in silico* analyses relied on structures to predict most toxic endpoints using structural alerts (SAs) [44]. However, SAs utilize binary features and qualitative endpoints, which can lead to incomplete and inaccurate predictions. The list of SAs and rules is potentially incomplete, resulting in possible false negatives or positives in the predictions. This underscores the need for optimization and enhancement of these predictive models, as accurate mutagenicity and genotoxic assessments are crucial for evaluating human health risks [45].

Arbutin was not predicted as a skin sensitizer, what possibilities for its notorious use in the cosmetology field, being used in skin care treatments [46]. The evaluation of the selective cytotoxic of the compounds on cancer cell lines exhibited that the three molecules have an important effect against tumor cell lines, a necessary attribute for new drugs in the treatment of cancer [30].

Analysing the other parameters, no harm was observed according to the prediction, this has importance for the preliminary risk assessment. Predictions of the LOAEL (Lowest Observed Adverse Effect Level) and LD50 (Lethal Dose for 50 %) serve as crucial tools in refining animal testing protocols, ensuring the administration of more accurate doses in the assays. [12]. The lowest LOAEL and LD50 are from Dihydroformononetin, indicating that this molecule can induce an adverse effect in a lower dose, needing more caution in the dosage than Arbutin and Caffeic Acid 4-O-glucoside.

It is possible to notice the downregulation of genes involved in the regulation of Wnt signal transduction, is important for the regulation of nuclear transcription. Arbutin downregulates *GSK3B*, *APC*, and *AXIN1*; Caffeic acid 4-O-glucoside downregulates *APC* and *AXIN*. As seen, APC needs a low binding energy of 6.9 and −6.8 kcal/mol, respectively. These genes are involved in the destruction complex of B-catenin. In this sense, it is possible to notice that *CTNNB1*, a gene responsible for B-catenin expression, is upregulated by Arbutin and Caffeic acid 4-O-glucoside and shows a high binding affinity, of −7.5 and −5.3 kcal/mol, respectively. Together they can increase the levels of B-catenin in

Table 4
Comparison between pKCSM and LAZAR toxicity prediction.

	Model Name	pKCMS		LAZAR	
		Unit	Prediction	Unit	Prediction
Arbutin	AMES toxicity	Categorical (Yes/No)	No	Categorical (Yes/No)	Yes
	hERG inhibitor	Categorical (Yes/No)	No	n.a.	—
	Oral Rat Acute Toxicity (LD50)	Numeric (mol/kg)	1.641	n.a.	—
	Oral Rat Chronic Toxicity (LOAEL)	Numeric (mg/kg/day)	3.140	Regression (mg/kg/day)	871
	Carcinogenicity (Rodents)	n.a.	—	Categorical (Yes/No)	No
	Hepatotoxicity	Categorical (Yes/No)	No	n.a.	—
	Skin Sensitisation	Categorical (Yes/No)	No	n.a.	—
	Max. tolerated dose (human)	Numeric (mg/kg/day)	3.07	Numeric (mg/kg/day)	33.7
Caffeic acid 4-O-glucoside	AMES toxicity	Categorical (Yes/No)	No	Categorical (Yes/No)	No
	hERG inhibitor	Categorical (Yes/No)	No	n.a.	—
	Oral Rat Acute Toxicity (LD50)	Numeric (mol/kg)	2.579	n.a.	—
	Oral Rat Chronic Toxicity (LOAEL)	Numeric (mg/kg/day)	11.428	n.a.	—
	Carcinogenicity (Rodents)	n.a.	—	Categorical (Yes/No)	No
	Hepatotoxicity	Categorical (Yes/No)	No	n.a.	—
	Skin Sensitisation	Categorical (Yes/No)	No	n.a.	—
	Max. tolerated dose (human)	Numeric (mg/kg/day)	3.273	Numeric (mg/kg/day)	15.1
Dihydroformononetin	AMES toxicity	Categorical (Yes/No)	Yes	Categorical (Yes/No)	No
	hERG inhibitor	Categorical (Yes/No)	No	n.a.	—
	Oral Rat Acute Toxicity (LD50)	Numeric (mol/kg)	2.342	n.a.	—
	Oral Rat Chronic Toxicity (LOAEL)	Numeric (mg/kg/day)	103.5	Regression (mg/kg/day)	102
	Carcinogenicity (Rodents)	n.a.	—	Categorical (Yes/No)	No
	Hepatotoxicity	Categorical (Yes/No)	No	n.a.	—
	Skin Sensitisation	Categorical (Yes/No)	No	n.a.	—
	Max. tolerated dose (human)	Numeric (mg/kg/day)	1.67	Numeric (mg/kg/day)	6.67

hERG: human Ether-a-go-go-Related Gene; LD50: lethal dose of 50 %; LOAEL: lowest observed adverse effect level.

Table 5
Toxicological prediction through structural alerts of ToxTree.

	Carcinogenicity	Micronucleus	Mutagenicity (Ames)
Arbutin	No alerts	At least one	No alerts
DHFN	No alerts	At least one	No alerts
Caffeic acid 4-O-glucoside	No alerts	At least one	No alerts

Table 6
Cytotoxicity prediction of CLC-pred.

	Tumoral	Non-tumoral
Arbutin	111	9
DHFN	51	10
Caffeic acid 4-O-glucoside	77	6

the cytoplasm and so, the nuclear transcription. However, the deregulated activation of the Wnt pathway is associated with the generation of human tumors [47,48]. Even so, some studies exhibited that Wnt signaling may act as a tumor suppressor by interfering in the differentiation of tumor cell lines in the mature lineage [49]. It was shown that the stimulation of this pathway in osteosarcoma cell lines inhibits cell proliferation and differentiation, indicating its role as a tumor suppressor, what can lead to beneficial impacts [50].

NEDD8, a gene responsible for neddylation and crucial in proteasomal degradation, operates alongside *RBX1*, a regulator of this process [51]. Notably, both have emerged as promising targets for anticancer therapies. Inhibition of NEDD8 has shown considerable efficacy in *in vivo* studies of neuroblastoma, while RBX1's pivotal role in cell proliferation and its association with poor prognosis in esophageal and gastric cancers underscore its significance [52,53]. Remarkably, Arbutin downregulates both *NEDD8* and *RBX1*, suggesting a potential mechanism for its antitumoral effects. In docking studies, NEDD8 exhibits a binding affinity of −5.8 kcal/mol, indicating a potential disruption in neddylation-mediated processes. Similarly, RBX1 demonstrates a binding energy of −6.4 kcal/mol, further supporting its role in Arbutin-mediated effects on cancer-related pathways.

NEDD8 has become a focal point for developing anticancer drugs. Its downregulation significantly suppressed tumor growth *in vitro* and *in vivo*, inducing cell cycle arrest, DNA damage, and apoptosis in

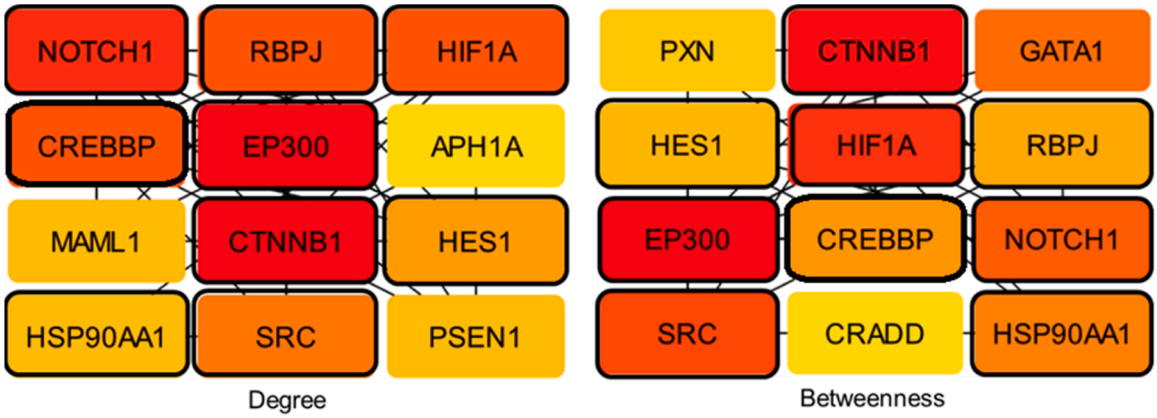

Fig. 3. Arbutin Upregulation Centrality Measures. In black, the hub-bottleneck genes.

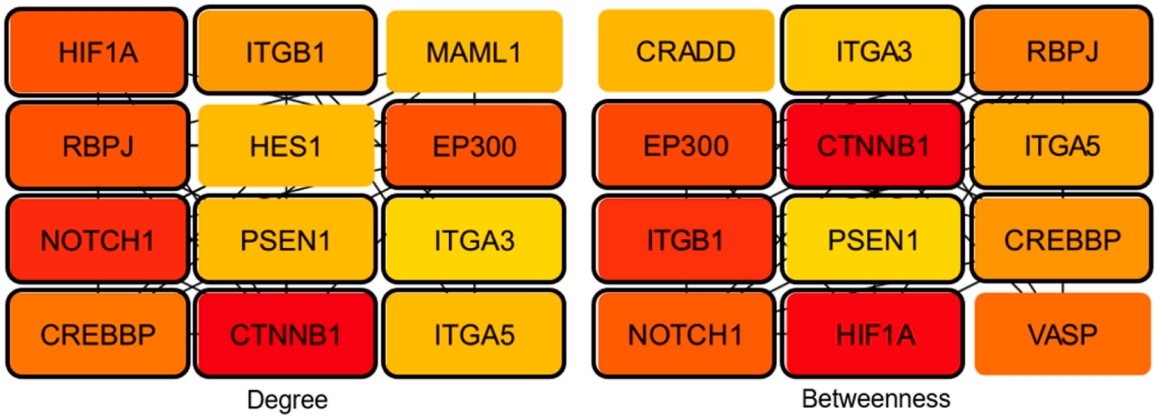

Fig. 4. Caffeic acid 4-O-glucoside Upregulation Centrality Measures. In black, the hub-bottleneck genes.

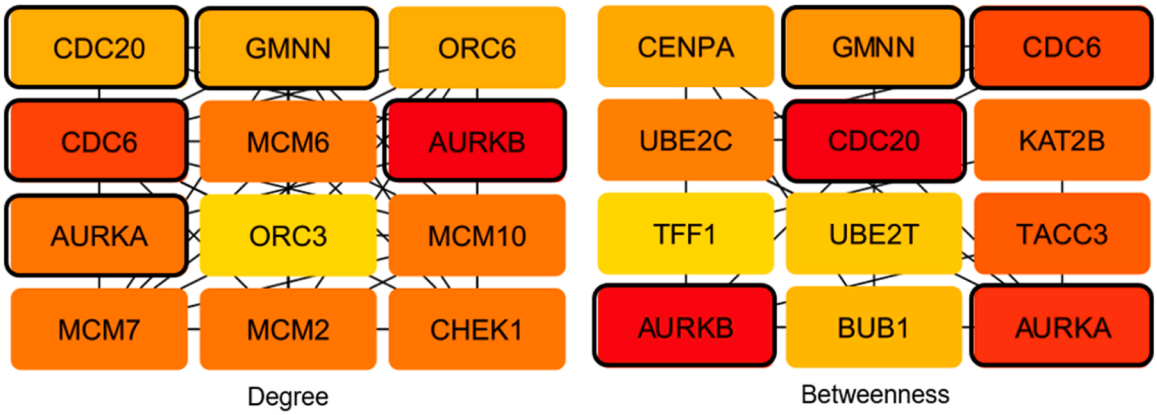

Fig. 5. Dihydroformononetin Upregulation Centrality Measures In black, the hub-bottleneck genes.

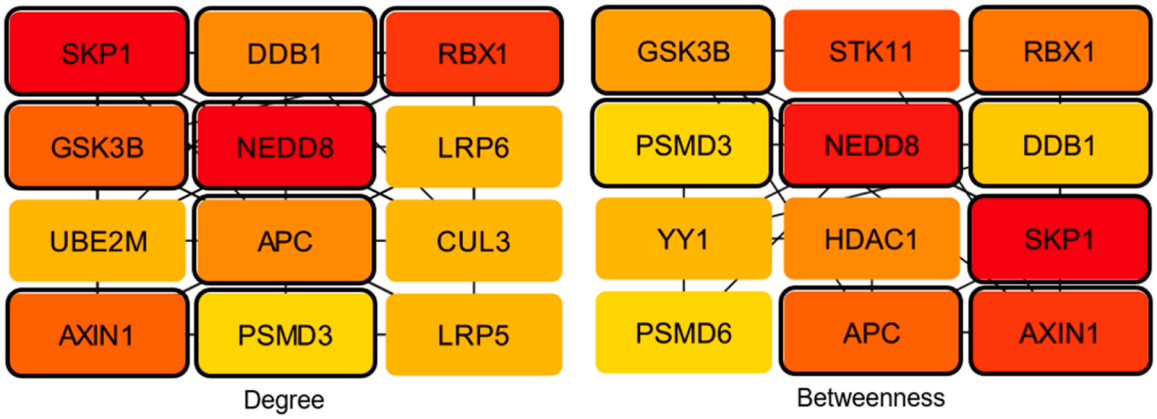

Fig. 6. Arbutin Downregulation Centrality Measures. In black, the hub-bottleneck genes.

esophageal squamous cell carcinoma (ESCC) cells [54,55]. Conversely, RBX1 overexpression correlates with poor outcomes in patients with triple-negative breast cancer (TNBC), promoting TNBC cell metastasis both *in vitro* and *in vivo* [56]. These findings underscore the intricate regulatory networks influenced by Arbutin and highlight the potential therapeutic implications of targeting NEDD8 and RBX1 in cancer treatment strategies.

The gene *DDB1* codifies the Damage DNA-binding protein 1, which operates in DNA repair. The deletion of this gene, downregulated by Arbutin and with a low binding energy of −7.0 kcal/mol, can promote tumor through cell proliferation and increase chemoresistance, as observed in pancreatic adenocarcinoma [57]. Another gene undergoing downregulation is SKP1, a prime target in cancer therapy. Its elevation correlates with unfavorable prognosis in colon cancer patients [51], underscoring the significance of seeking methods to reduce SKP1 expression. PSMD3 is a member of the proteasome family and is upregulated in breast cancer, which is linked to the shorter overall survival of the patients [58]. *HDAC1* codifies histone deacetylase 1. The overexpression of this gene is related to resistance in cancer therapies [59]. The downregulation of *DDB1*, *SKP1*, *PSMD3*, and *HDCA1* shows interesting mechanisms to be exploited for the treatment of cancer.

HIF1α is upregulated by Arbutin and Caffeic acid 4-O-glucoside. Its

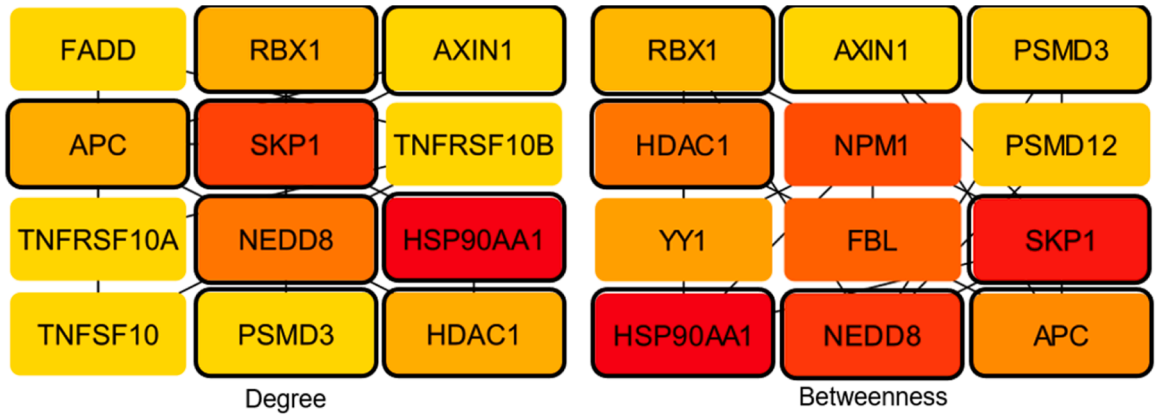

Fig. 7. Caffeic acid 4-O-glucoside Downregulation Centrality Measures. In black, the hub-bottleneck genes.

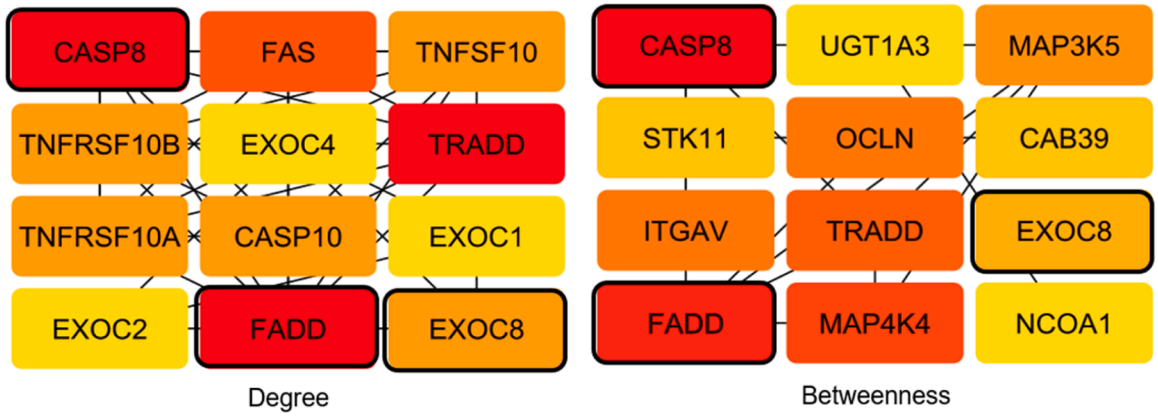

Fig. 8. Dihydroformononetin Downregulation Centrality Measures. In black, the hub-bottleneck genes.

protein has a binding energy of −5.7 kcal/mol with Arbutin and −5.5 kcal/mol by Caffeic acid 4-O-glucoside. This gene becomes active to promote cellular survival during hypoxic conditions, enhancing the expression of certain genes. Its interaction with signaling pathways such as Notch and Wnt, as previously mentioned, is well-established, and the great binding affinity displayed by the molecular docking emphasizes this relation [60]. While this gene is linked to cancer progression and development, it has been noted that the upregulation of Notch-Hifα plays a significant role in liver regeneration [61]. *NOTCH1*, a gene upregulated by Arbutin and Caffeic acid 4-O-glucoside too, has different roles in cancer development. NOTCH1 has high binding affinity with Arbutin (-6.5 kcal/mol) and Caffeic acid 4-O-glucoside (-6.4 kcal/mol), and this protein exhibits dual roles in cancer development, functioning as either a tumor suppressor or an oncogene depending on tissue context [62]. *HES1*, upregulated gene, is also a target for NOTCH, and its expression is increased in hypoxia, thus, associated with Notch-Hifα. Just like them, HES1 is overexpressed in breast cancer, contributing to cell proliferation [63]. RBPJ is an important regulator of the NOTCH pathway, activating the signalization when bound to NOTCH proteins. This gene, as *NOTCH1*, is upregulated by the same two molecules, and, as previously seen, its loss promotes tumorigenesis [64,65]. *SRC*, another gene boosted by Arbutin, functions as an oncogene crucial for tumor growth and advancement [66]. These intricate binding energies show the complex molecular mechanisms modulated by Arbutin and Caffeic acid 4-O-glucoside, implicating multiple pathways in their potential therapeutic effects.

EP300 and *CREBBP* are critical tumor suppressors with significant roles in cancer biology. Our *in silico* results predicted that *EP300* is upregulated by both Arbutin and Caffeic acid 4-O-glucoside, and its protein has a binding energies lower than −6.0 kcal/mol in both cases. EP300, known for regulating cell adhesion, apoptosis, and stemness, has been previously shown to be downregulated in breast cancer [67]. Upregulation of *EP300*, as predicted in our study, could therefore be beneficial for cancer treatment due to its tumor-suppressive functions.

Similarly, CREBBP, which promotes the activity of other tumor suppressors like p53 and RB1 [68], was predicted to be upregulated by both molecules too. The molecular docking showed a high binding affinity of −6.6 kcal/mol with Caffeic acid 4-O-glucoside. CREBBP's role in stimulating the transcription of p53, particularly following DNA damage, underscores its importance in maintaining genomic stability and preventing tumorigenesis [69]. The predicted upregulation of these genes aligns with their established roles in tumor suppression, suggesting a potential therapeutic benefit of Caffeic acid 4-O-glucoside and Arbutin in cancer treatment. These findings are promising as they indicate that these compounds could positively influence key tumor suppressor pathways. The strong binding affinities observed further support the potential effectiveness of these compounds.

PSEN1 is a gene highly associated with Alzheimer's disease. This gene codifies presenilin 1, required for neural development. This gene showed a suppressor role in the chemoresistance of Bladder cancer [70], sensitizing cells to the treatment. *PSEN1* is upregulated by Caffeic acid 4-O-glucoside, exhibiting the potential to interfere positively in treatments with chemoresistance.

Genes that are members of the integrin family, *ITGA3*, *ITGA5*, and *ITGB1* are upregulated by Caffeic acid 4-O-glucoside and these integrins have binding energy lower than −7.0 kcal/mol. They are important for cytoskeletal organization and cell survival [71]. These integrins are upregulated in some types of cancer. *ITGA3* knockdown by miR199a-5p

Table 7
The docking interactions characteristics of Arbutin with hit ligands.

Ligand	Binding energy (kcal/mol)	Expression status	H-Bond	Other non-covalent interactions
CTNNB1	−7.5	UP	ASN121, PRO119, HIS118	ARG124, ALA145, ASP146, ARG194, LEU150, THR120, MET190, LYS149, LYS193
EP300	−6.1	UP	GLU564, GLN873, HIS839	GLN561, LEU566, SER565, GLN842, LEU883, ARG 838, VAL878, ASP837, SER881, ASN875, ARG927
HES1	−4.2	UP	ASN43, TYR8	ARG36, HIS40, GLN47, GLY11, ALA10, LYS7, CYS44, GLU14
HIF1A	−5.7	UP	GLN148, SER91, THR149, GLN147	ILE806, SER184, GLN814, TYR93, TYR102, ASN803, ALA804, PRO805, LEU186
HSP90AA1	−6.8	UP	ASN106, SER52	ASP102, LEU107, PHE138, VAL186, ASN51, THR184, ASP93, ASP54, LYS58, MET98
NOTCH1	−6.5	UP	ASN24, GLY329, GLU328, GLY65	GLU28, ALA21, MET330, TYR327, GLY331, GLN32, LYS68, LYS69, ARG75, GLN72
RBPJ	−5.7	UP	EDO507, GLN402, GLU363	EDO510, TYR364, ALA362, BU1522, LYS361, LYS185, VAL382, GLU384
SRC	−5.2	UP	LYS109, HIS107, ARG86, SER88	PHE108, ARG67, SER96, ASP94, LEU111
APC	−6.9	DOWN	ARG606	PHE23, SER103, GLY105, GLN18, VAL21, GLU19, LYS104, ALA112, LYS107, ASP90, ARG594, GLU91, LEU76, GLU92, PHE20
AXIN1	−5.2	DOWN	HIS127, GLN223, GLN227, GLU231	-
DDB1	−7.0	DOWN	ALA82, HIS1077, ARG111, GLY113, THR1078,	ARG1080, ARG570, ILE112, SER567, TYR84, ARG114, PRO115, GLN109, GLU1079
NEDD8	−5,1	DOWN	SER65, TYR45	SER46
PSMD3	−6.4	DOWN	ARG926	LYS860, ALA861
RBX1	−4.9	DOWN	ASN41, VAL38	ILE37, ALA43, ASP36, LEU96, PRO95, TRP35, ARG46
SKP1	−6.0	DOWN	SER139, ASP81, IHP601	ARG114, GLU165, SER138, LYS113, ARG164, ARG334, ARG403

Table 8
The docking interactions characteristics of Caffeic Acid 4-O-glucoside with hit ligands.

Ligand	Binding energy (kcal/mol)	Expression status	H-Bond	Other non-covalent interactions
CREBBP	−6.6	UP	SER1179, ARD1112	SER1136, GLU1183
CTNNB1	−5.3	UP	HIS499, GLU310,*	ASN308, LYS496,*
EP300	−6.3	UP	SER565, GLN529, ASP571, LEU528,*	LEU566, ASN527,*
HIF1A	−5.5	UP	ALA198	LEU101, VAL242, TYR230, SER240, THR97, PHE244, HIS199, ARG117, PHE114, PRO197, GLN239, ASP243, LYS99,*
ITGA3	−8.1	UP	GLU240, PHE238	LYS250, LEU222, HIS261, ARG246, ALA244
ITGA5	−7.0	UP	SER134, LEU225, ASN224, SER132, GLU229	PHE187, SER224, SER227
ITGB1	−7.4	UP	ASN288, LYS300, LYS303, GLU285	LEU304,*
NOTCH1	−6.4	UP	GLN74, GLU328	ALA21
PSEN	−5.6	UP	GLU184,*	TYR181
RBPJ	−7.2	UP	CYS278, VAL231, LYS212, TRP243,*	LEU77, VAL280, ALA245,*
APC	−6.8	DOWN	ASP252, LEU249, ASN250, CYS150, ARG77	-
AXIN1	−5.9	DOWN	THR224, ARG162	-
HDAC1	−5.6	DOWN	LYS91, LYS88, ARG71, ARG119,*	GLN124,*
HSP90AA1	−5.5	DOWN	GLU227, GLU332, ASN238	ARG222, MET285
NEDD8	−5.8	DOWN	ARG342. THR9, PRO338, GLN341, LYS327,*	GLY110, GLN339, ALA372,*
PSMD3	−6.7	DOWN	ARG856, ARG926, ASP924	-
RBX1	−6.4	DOWN	ASN41, VAL38	ALA43, LEU96
SKP1	−6.7	DOWN	SER510, LYS485, ARG484, LYS113	ARG509

* Other unknown bindings.

suppressed the proliferation, migration, and invasion in cases of colorectal cancer, but when it is overexpressed, unfortunately these effects are restored [72]. *ITGA5* is upregulated in oral squamous carcinoma, this role was explained by its contribution to epithelial-mesenchymal transition (EMT) [73]. These two alpha integrins are upregulated too in head and neck squamous cell carcinoma [71]. *ITGB1* is upregulated in hepatocellular carcinoma (HCC), activating PXN and YWHAZ, molecules associated with HCC tumor cell cycle progression, driving the cell cycle acceleration [74]. The role of these integrins in cancer

Table 9
The docking interactions characteristics of Dihydroformononetin with hit ligands.

Ligand	Binding energy (kcal/mol)	Expression status	H-Bond	Other non-covalent interactions
AURKA	−7.1	UP	-	VAL147, LEU263
AURKB	−8.9	UP	-	ALA217, LEU83, LEU207, PHE88
CDC6	−7.0	UP	-	ARG237, ILE345, ASN352
CDC26	−7.2	UP	LEU449	SER448, ASN188, VAL190, ARG316, VAL232, ASP191, ALA233, SER275, TRP276, TRP234, LEU406, LYS359, LEU447, SER404
GMNN	−5.1	UP		GLU125, HIS121
CASP8	−6.8	DOWN	-	ARG337, TRP403, HIS334, LEU333, TRP466, LEU405
EXOC8	−6.8	DOWN	-	GLY171, ALA274, LYS278, LEU275, TYR173
FADD	−5.9	DOWN	-	LEU172, ILE295, LYS296

development is crucial and when upregulated, like by Caffeic acid 4-O-glucoside, it can enhance cancer cells growth.

The Cell Division Cycle (CDC) genes are pivotal in DNA replication initiation and cell division regulation. While inhibiting CDC20 has shown promise in suppressing metastasis in triple-negative breast cancer [75], Dihydroformononetin, upregulates its expression. Similarly, CDC6, associated with cancer development due to its abnormal expression [76], is also upregulated by Dihydroformononetin, indicating potential implications for cell cycle dynamics. Moreover, Dihydroformononetin upregulates AURKA and AURKB, members of the Aurora kinase family crucial for mitosis regulation, with notably low binding energies, indicating strong binding affinity. Particularly, AURKB, responsible for kinetochore formation essential for proper chromosome disjunction, when upregulated, may safeguard against abnormal cell division, aligning with predictions of reduced micronuclei formation [77]. AURKB exhibits upregulation with a high binding affinity of −8.9 kcal/mol, underscoring its potential role in Dihydroformononetin-mediated effects on cell division regulation. AURKA, with a binding energy of −7.1 kcal/mol, further supports the intricate regulatory network influenced by Dihydroformononetin. The upregulation of these genes protect from abnormal division [77]. This aligns with the prediction of the absence of micronuclei, as illustrated in Table 5.

FADD and *CASP8* are genes directly involved in the regulation of apoptosis and inflammation control and are downregulated by Dihydroformononetin. Together, they are essential for death receptor-induced apoptosis and the induction of proinflammatory responses [78,79]. Our in silico docking analysis revealed that CASP8 showed a high binding affinity with Dihydroformononetin, with a binding energy of −6.8 kcal/mol, while FADD had a binding energy of −5.9 kcal/mol. These strong interactions suggest that Dihydroformononetin could

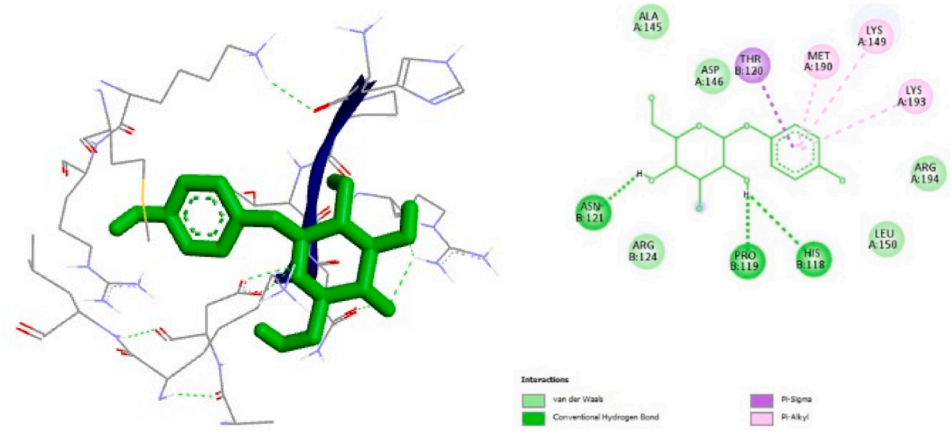

Fig. 9. 3D and 2D representations of ligand–protein interactions between Arbutin and the active site of CTNNB1.

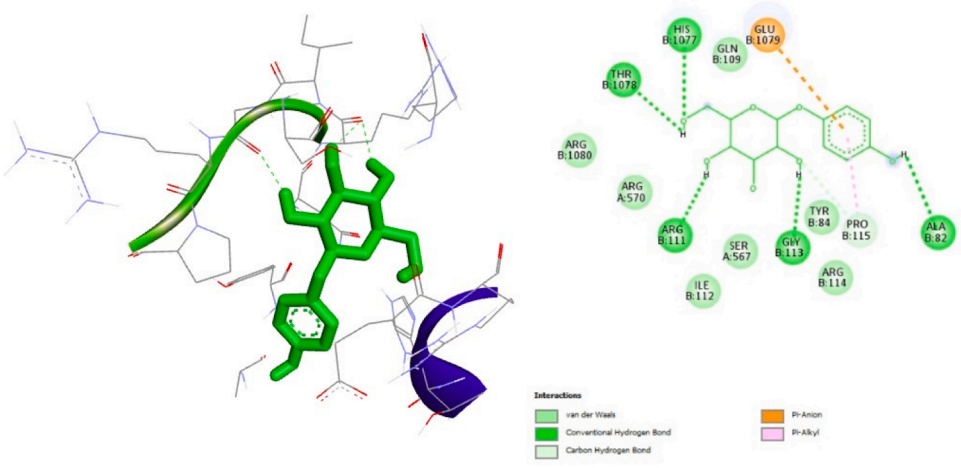

Fig. 10. 3D and 2D representations of ligand–protein interactions between Arbutin and the DDB1 active site.

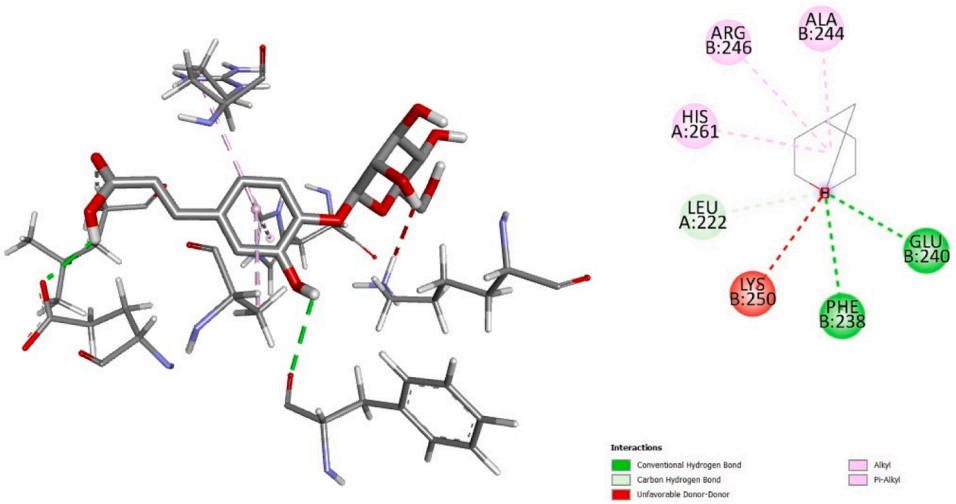

Fig. 11. 3D and 2D representations of ligand–protein interactions between Caffeic Acid 4-O-glucoside and the ITGA3 active site.

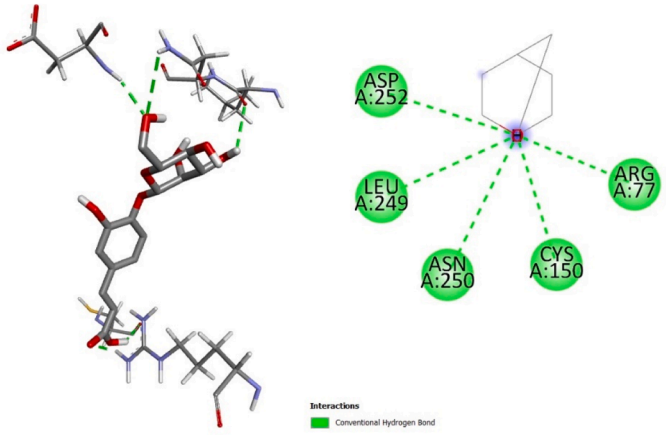

Fig. 12. 3D and 2D representations of ligand–protein interactions between Caffeic Acid 4-O-glucoside and the APC active site.

effectively modulate their activity. Given that the extract of *Cyrtopodium glutiniferum* demonstrated anti-inflammatory properties in our previous studies [10], the negative modulation of *CASP8* and *FADD* by Dihydroformononetin may explain these anti-inflammatory effects. The downregulation of these genes could reduce proinflammatory responses and apoptosis, contributing to the extract's therapeutic potential. This highlights the importance of Dihydroformononetin in the pharmacological effects of *Cyrtopodium glutiniferum* and supports further investigation into its mechanisms of action.

HSP90AA1 gene codifies the Heat shock protein 90-alpha. This chaperone is mainly expressed in tumors, infections, and trauma. The HSP family of proteins is present in immune and inflammatory processes [80]. *HSP90AA1* is upregulated in some types of cancer, and its inhibition was capable of promoting anti-tumor immunity, being an important target in cancer research [81]. In the gene regulation prediction, it was seen that *HSP90AA1* is upregulated by Arbutin but downregulated by Caffeic acid 4-O-glucoside. Its upregulation must be seen carefully, and the downregulation shows great potential for cancer therapeutics and may justify the anti-inflammatory activity.

While the *in silico* analyses provide valuable insights into the therapeutic potential of compounds from *Cyrtopodium glutiniferum*, they come with limitations. The reliance on theoretical models such as SARs and QSARs can result in inaccurate predictions, as seen in the divergent mutagenicity results for Arbutin and Dihydroformononetin [44]. Additionally, it is important to have experimental validation to confirm the biological relevance of the high binding affinities observed in our docking studies. The prediction platforms used may also have incomplete databases, affecting the accuracy of our results. Therefore, supplementing these findings with experimental studies *in vitro* and *in vivo* remains essential for a thorough understanding of the pharmacokinetics, toxicological profiles, and molecular interactions of these compounds, thus establishing a robust foundation for developing new therapeutic agents. Furthermore, utilizing the insights obtained from the *in silico* approach can offer valuable direction for subsequent investigations,

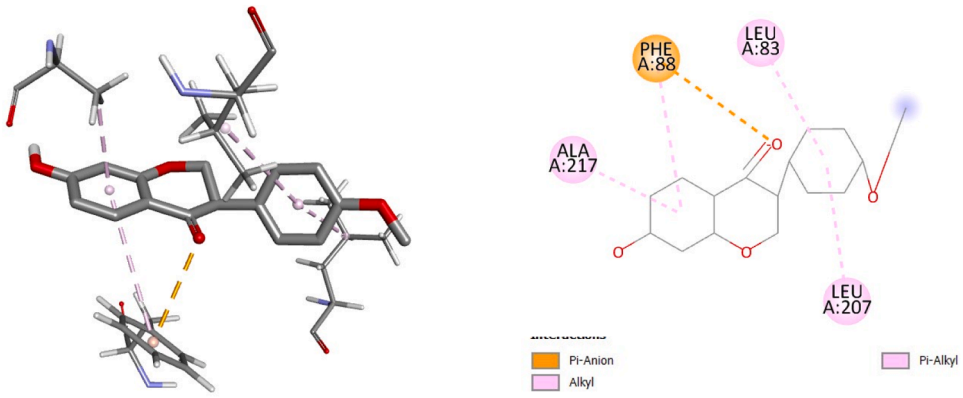

Fig. 13. 3D and 2D representations of ligand–protein interactions between Dihydroformononetin and the AURKB active site.

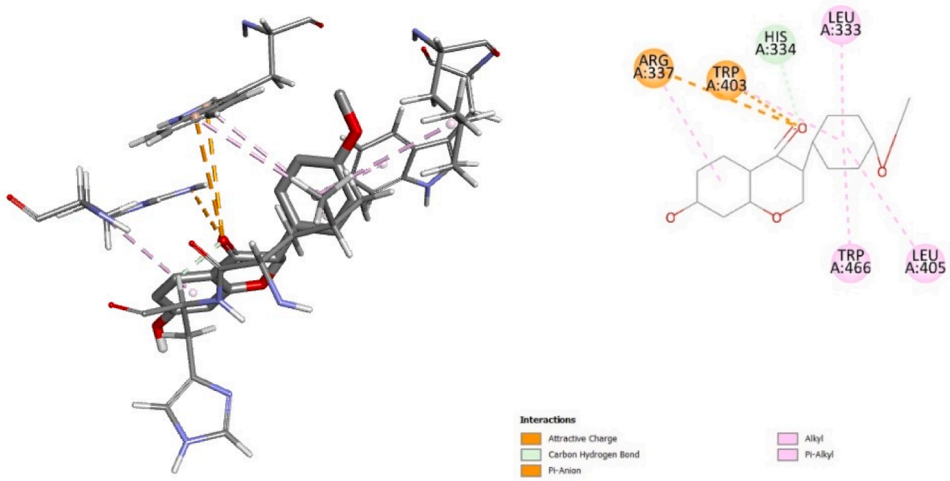

Fig. 14. 3D and 2D representations of ligand–protein interactions between Dihydroformononetin and the CASP8 active site.

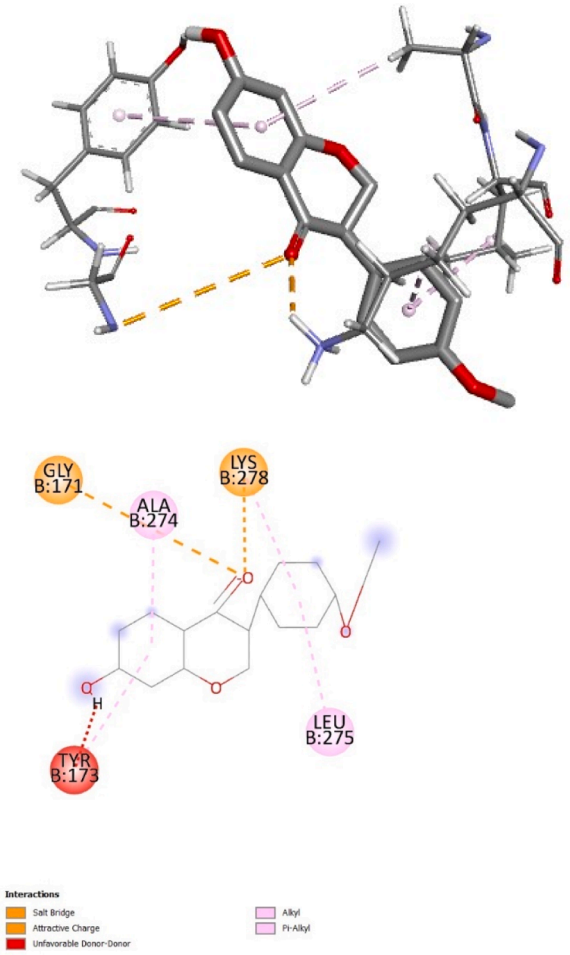

Fig. 15. 3D and 2D representations of ligand–protein interactions between Dihydroformononetin and the EXOC8 active site.

aiding in the identification of optimal targets and potentially minimizing time and resource consumption in the drug development process.

Together, these predictions underscore the potential of Arbutin, Caffeic Acid 4-O-glucoside, and Dihydroformononetin as promising candidates for the development of novel therapeutics, particularly in areas such as anti-inflammatory agents and cancer therapeutics. Given the convergence in their targets, Arbutin and Caffeic Acid 4-O-glucoside may potentially exhibit synergistic effects when combined, enhancing their overall therapeutic efficacy. However, it is imperative to note that important aspects such as their absorption, mutagenicity, and interaction with Cytochrome P450 enzymes still need further analysis. These molecules were shown to interfere with the gene expression of significant pathways, including Wnt. Dihydroformononetin downregulates proinflammatory genes, indicating anti-inflammatory potential, as seen in the *Cyrtopodium glutiniferum* extract. They demonstrated great binding energy with the respective proteins observed in DIGEP. To validate these findings and better understand the results of these gene interactions, more *in vitro* and *in vivo* studies are necessary, ultimately supporting the therapeutic potential of these bioactive compounds.

CRediT authorship contribution statement

Natália Gonçalves Ribeiro Araujo: Writing – original draft, Visualization, Methodology, Investigation, Formal analysis, Data curation, Conceptualization. **Francisco Carlos da Silva Junior:** Writing – original draft, Validation, Methodology, Investigation, Formal analysis. **Lizandra Vitória de Souza Santos:** Methodology, Investigation, Formal analysis, Data curation, Conceptualization. **Silvia Regina Batistuzzo de Medeiros:** Writing – review & editing, Validation, Supervision. **Israel Felzenszwalb:** Writing – review & editing, Supervision, Resources, Funding acquisition. **Carlos Fernando Araújo-Lima:** Writing – review & editing, Supervision, Resources, Project administration, Funding acquisition.

Declaration of Competing Interest

The authors declare that they have no known competing financial interests or personal relationships that could have appeared to influence the work reported in this paper.

Acknowledgements

This work was supported by Coordination of Superior Level Staff Improvement (CAPES) (Code 0001); National Council for Scientific and Technological Development – CNPq [408259/2023-0-CFA-L; 302345/2017-5-IF; 165757/2021-3-NGRA] and The Carlos Chagas Filho Foundation for Research Support of the State of Rio de Janeiro (FAPERJ) [E-26/202.759/2017- IF; E-26/210.096/2023-CFA-L and IF]. The authors thank Living Skies Scholarship Program, University of Saskatchewan, Canada [FCSJ – Postdoctoral Fellowship]. The Carlos Chagas Filho Foundation for Research Support of the State of Rio de Janeiro FAPERJ

N°13/2023 – Auxílio Básico à Pesquisa (APQ1) – 2023.

Appendix A. Supporting information

Supplementary data associated with this article can be found in the online version at doi:10.1016/j.toxrep.2024.101810.

Data availability

Data will be made available on request.

References

[1] A.L. Harvey, Natural products in drug discovery, Drug Discov. Today 13 (2008) 894–901, https://doi.org/10.1016/j.drudis.2008.07.004.

[2] M. Akram, M. Riaz, A.W.C. Wadood, A. Hazrat, M. Mukhtiar, S. Ahmad Zakki, M. Daniyal, M.A. Shariati, F. Said Khan, R. Zainab, Medicinal plants with anti-mutagenic potential, Biotechnol. Biotechnol. Equip. 34 (2020) 309–318, https://doi.org/10.1080/13102818.2020.1749527.

[3] D.J. Newman, G.M. Cragg, Natural products as sources of new drugs from 1981 to 2014, J. Nat. Prod. 79 (2016) 629–661, https://doi.org/10.1021/acs.jnatprod.5b01055.

[4] T.H. Nguyen-Vo, L. Nguyen, N. Do, T.N. Nguyen, K. Trinh, H. Cao, L. Le, Plant metabolite databases: from herbal medicines to modern drug discovery, J. Chem. Inf. Model. 60 (2020) 1101–1110, https://doi.org/10.1021/acs.jcim.9b00826.

[5] S. Sut, F. Maggi, S. Dall, Acqua, Bioactive secondary metabolites from orchids (Orchidaceae), Chem. Biodivers. 14 (2017) e1700172, https://doi.org/10.1002/cbdv.201700172.

[6] V. Morales-Sánchez, I. Rivero-Cruz, G. Laguna-Hernández, G. Salazar-Chávez, R. Mata, Chemical composition, potential toxicity, and quality control procedures of the crude drug of cyrtopodium macrobulbon, J. Ethnopharmacol. 154 (2014) 790–797, https://doi.org/10.1016/j.jep.2014.05.006.

[7] F. Auberon, O.J. Olatunji, G. Herbette, D. Raminoson, C. Antheaume, B. Soengas, F. Bonté, A. Lobstein, Chemical constituents from the aerial parts of cyrtopodium paniculatum, Molecules 21 (2016) 1–18, https://doi.org/10.3390/molecules21101418.

[8] E.S. Teoh, Orchids as Aphrodisiac, Medicine Or Food, Springer Nature, 2019, pp. 159–171, 10.1007/978-3-030-18255-7.

[9] D.W. Barreto, J.P. Parente, Chemical properties and biological activity of a polysaccharide from cyrtopodium cardiochilum, Carbohydr. Polym. 64 (2006) 287–291, https://doi.org/10.1016/j.carbpol.2005.11.038.

[10] C.F. Araujo-Lima, I. Felzenszwalb, A.F. Macedo, Cyrtopodium glutiniferum, an example of orchid used in folk medicine: phytochemical and biological aspects, : Orchid. Phytochem. Biol. Hortic. (2021) 1–16, https://doi.org/10.1007/978-3-030-11257-8_33-1.

[11] C.F. Araújo-Lima, J. Paula da Silva Oliveira, I.L. Coscarella, C.A.F. Aiub, I. Felzenszwalb, G.P. Caprini Evaristo, A.F. Macedo, Metabolomic analysis of cyrtopodium glutiniferum extract by UHPLC-MS/MS and in vitro antiproliferative and genotoxicity assessment, J. Ethnopharmacol. 253 (2020) 112607, https://doi.org/10.1016/j.jep.2020.112607.

[12] K.T. Rim, In silico prediction of toxicity and its applications for chemicals at work, Toxicol. Environ. Health Sci. 12 (2020) 191–202, https://doi.org/10.1007/s13530-020-00056-4.

[13] F. Badalà, K. Nouri-mahdavi, D.A. Raoof, Recent advances in ligand-based drug design: relevance and utility, Comput. (Long. Beach Calif.) 144 (2008) 724–732.

[14] G. Gini, QSAR methods (2022) 1–26, https://doi.org/10.1007/978-1-0716-1960-5_1.

[15] M. Saeedi, K. Khezri, A. Seyed Zakaryaei, H. Mohammadamini, A comprehensive review of the therapeutic potential of α-arbutin, Phyther. Res. 35 (2021) 4136–4154, https://doi.org/10.1002/ptr.7076.

[16] Y.C. Boo, Arbutin as a skin depigmenting agent with antimelanogenic and antioxidant properties, Antioxidants 10 (2021) 1–22, https://doi.org/10.3390/antiox10071129.

[17] C. Ma, D. Zhang, Q. Ma, Y. Liu, Y. Yang, Arbutin inhibits inflammation and apoptosis by enhancing autophagy via SIRT1, Adv. Clin. Exp. Med. 30 (2021), https://doi.org/10.17219/ACEM/133493.

[18] Z.-Y. Yang, T. Kuboyama, K. Kazuma, K. Konno, C. Tohda, Active constituents from Drynaria fortunei rhizomes on the attenuation of Aβ 25–35 -induced axonal atrophy, J. Nat. Prod. 78 (2015) 2297–2300, https://doi.org/10.1021/acs.jnatprod.5b00290.

[19] H.-Y. Park, M. Kim, J. Han, Stereospecific microbial production of isoflavanones from isoflavones and isoflavone glucosides, Appl. Microbiol. Biotechnol. 91 (2011) 1173–1181, https://doi.org/10.1007/s00253-011-3310-7.

[20] K.-C. Tay, L.T.-H. Tan, C.K. Chan, S.L. Hong, K.-G. Chan, W.H. Yap, P. Pusparajah, L.-H. Lee, B.-H. Goh, Formononetin: a review of its anticancer potentials and mechanisms, Front. Pharmacol. 10 (2019), https://doi.org/10.3389/fphar.2019.00820.

[21] C. Ma, R. Xia, S. Yang, L. Liu, J. Zhang, K. Feng, Y. Shang, J. Qu, L. Li, N. Chen, S. Xu, W. Zhang, J. Mao, J. Han, Y. Chen, X. Yang, Y. Duan, G. Fan, Formononetin attenuates atherosclerosis via regulating interaction between KLF4 and SRA in apoE -/- mice, Theranostics 10 (2020) 1090–1106, https://doi.org/10.7150/thno.38115.

[22] J.M. Dutra, P.J.P. Espitia, R.A. Batista, Formononetin: biological effects and uses – A review, Food Chem. 359 (2021), https://doi.org/10.1016/j.foodchem.2021.129975.

[23] L. Liao, L. Huang, X. Wei, L. Yin, X. Wei, T. Li, Bioinformatic and biochemical studies of formononetin against liver injure, Life Sci. 272 (2021), https://doi.org/10.1016/j.lfs.2021.119229.

[24] L. Nahar, A. Al-Groshi, A. Kumar, S.D. Sarker, Arbutin: occurrence in plants, and its potential as an anticancer agent, Molecules 27 (2022) 8786, https://doi.org/10.3390/molecules27248786.

[25] A. Masyita, E. Salim, R.M. Asri, F. Nainu, A. Hori, R. Yulianty, M. Hatta, Y. Rifai, T. Kuraishi, Molecular modeling and phenoloxidase inhibitory activity of arbutin and arbutin undecylenic acid ester, Biochem. Biophys. Res. Commun. 547 (2021) 75–81, https://doi.org/10.1016/j.bbrc.2021.02.006.

[26] S. Kim, J. Chen, T. Cheng, A. Gindulyte, J. He, S. He, Q. Li, B.A. Shoemaker, P. A. Thiessen, B. Yu, L. Zaslavsky, J. Zhang, E.E. Bolton, PubChem in 2021: new data content and improved web interfaces, Nucleic Acids Res. 49 (2021) D1388–D1395, https://doi.org/10.1093/nar/gkaa971.

[27] D.E.V. Pires, T.L. Blundell, D.B. Ascher, pkCSM: Predicting small-molecule pharmacokinetic and toxicity properties using graph-based signatures, J. Med. Chem. 58 (2015) 4066–4072, https://doi.org/10.1021/acs.jmedchem.5b00104.

[28] A. Daina, O. Michielin, V. Zoete, SwissADME: a free web tool to evaluate pharmacokinetics, drug-likeness and medicinal chemistry friendliness of small molecules, Sci. Rep. 7 (2017) 1–13, https://doi.org/10.1038/srep42717.

[29] A. Maunz, M. Gütlein, M. Rautenberg, D. Vorgrimmler, D. Gebele, C. Helma, Lazar: a modular predictive toxicology framework, Front. Pharmacol. 4 (2013) 1–10, https://doi.org/10.3389/fphar.2013.00038.

[30] A.A. Lagunin, V.I. Dubovskaja, A.V. Rudik, P.V. Pogodin, D.S. Druzhilovskiy, T. A. Gloriozova, D.A. Filimonov, N.G. Sastry, V.V. Poroikov, CLC-Pred: a freely available web-service for in silico prediction of human cell line cytotoxicity for drug-like compounds, PLoS One 13 (2018) 1–13, https://doi.org/10.1371/journal.pone.0191838.

[31] G. Patlewicz, N. Jeliazkova, R.J. Safford, A.P. Worth, B. Aleksiev, An evaluation of the implementation of the cramer classification scheme in the Toxtree software, SAR QSAR Environ. Res. 19 (2008) 495–524, https://doi.org/10.1080/10629360802083871.

[32] R. Benigni, C. Bossa, Mechanisms of chemical carcinogenicity and mutagenicity: a review with implications for predictive toxicology, Chem. Rev. 111 (2011) 2507–2536, https://doi.org/10.1021/cr100222q.

[33] R. Benigni, C. Bossa, O. Tcheremenskaia, Nongenotoxic carcinogenicity of chemicals: mechanisms of action and early recognition through a new set of structural alerts, Chem. Rev. 113 (2013) 2940–2957, https://doi.org/10.1021/cr300206t.

[34] A. Lagunin, S. Ivanov, A. Rudik, D. Filimonov, V. Poroikov, DIGEP-Pred: Web service for in silico prediction of drug-induced gene expression profiles based on structural formula, Bioinformatics 29 (2013) 2062–2063, https://doi.org/10.1093/bioinformatics/btt322.

[35] D. Szklarczyk, A.L. Gable, D. Lyon, A. Junge, S. Wyder, J. Huerta-Cepas, M. Simonovic, N.T. Doncheva, J.H. Morris, P. Bork, L.J. Jensen, C. von Mering, STRING v11: protein–protein association networks with increased coverage, supporting functional discovery in genome-wide experimental datasets, Nucleic Acids Res. 47 (2019) D607–D613, https://doi.org/10.1093/nar/gky1131.

[36] P. Shannon, A. Markiel, O. Ozier, N.S. Baliga, J.T. Wang, D. Ramage, N. Amin, B. Schwikowski, T. Ideker, Cytoscape: a software environment for integrated models of biomolecular interaction networks, Genome Res 13 (2003) 2498–2504, https://doi.org/10.1101/gr.1239303.

[37] C.H. Chin, S.H. Chen, H.H. Wu, C.W. Ho, M.T. Ko, C.Y. Lin, cytoHubba: identifying hub objects and sub-networks from complex interactome, BMC Syst. Biol. 8 (2014) 1–7, https://doi.org/10.1186/1752-0509-8-S4-S11.

[38] A.R. Borneman, J.A. Leigh-Bell, H. Yu, P. Bertone, M. Gerstein, M. Snyder, Target hub proteins serve as master regulators of development in yeast, Genes Dev. 20 (2006) 435–448, https://doi.org/10.1101/gad.1389306.

[39] H. Yu, P.M. Kim, E. Sprecher, V. Trifonov, M. Gerstein, The importance of bottlenecks in protein networks: correlation with gene essentiality and expression dynamics, PLoS Comput. Biol. 3 (2007) 713–720, https://doi.org/10.1371/journal.pcbi.0030059.

[40] D. Kim, J. Lee, S. Lee, J. Park, D. Lee, Predicting unintended effects of drugs based on off-target tissue effects, Biochem. Biophys. Res. Commun. 469 (2016) 399–404, https://doi.org/10.1016/j.bbrc.2015.11.095.

[41] A.M.X. Rodrigues, R.K.M. Costa, R.S. Machado, S.J.C. Gutierrez, F. das C.A. Lima, A.P. de Oliveira, In-silico studies of Riparin B in the design of drugs: physicochemical, pharmacokinetic and pharmacodynamic parameters In-silico, (2020). https://doi.org/10.1101/2020.04.24.059626.

[42] P. Manikandan, S. Nagini, Cytochrome P450 structure, function and clinical significance: a review, Curr. Drug Targets 19 (2017) 38–54, https://doi.org/10.2174/1389450118666170125144557.

[43] T.A. Jacobson, Comparative pharmacokinetic interaction profiles of pravastatin, simvastatin, and atorvastatin when coadministered with cytochrome P450 inhibitors, Am. J. Cardiol. 94 (2004) 1140–1146, https://doi.org/10.1016/j.amjcard.2004.07.080.

[44] J. Hemmerich, G.F. Ecker, In silico toxicology: from structure–activity relationships towards deep learning and adverse outcome pathways, WIREs Comput. Mol. Sci. 10 (2020), https://doi.org/10.1002/wcms.1475.

[45] G. Raitano, A. Roncaglioni, A. Manganaro, M. Honma, L. Sousselier, Q.T. Do, E. Paya, E. Benfenati, Integrating in silico models for the prediction of mutagenicity (Ames test) of botanical ingredients of cosmetics, Comput. Toxicol. 12 (2019) 100108, https://doi.org/10.1016/j.comtox.2019.100108.

[46] X. Zhu, Y. Tian, W. Zhang, T. Zhang, C. Guang, W. Mu, Recent progress on biological production of α-arbutin, Appl. Microbiol. Biotechnol. 102 (2018) 8145–8152, https://doi.org/10.1007/s00253-018-9241-9.
[47] M. Katoh, M. Katoh, Molecular genetics and targeted therapy of WNT-related human diseases (Review), Int. J. Mol. Med. (2017) 587–606, https://doi.org/10.3892/ijmm.2017.3071.
[48] G.G. Tortelote, R.R. Reis, F. de Almeida Mendes, J.G. Abreu, Complexity of the Wnt/β-catenin pathway: searching for an activation model, Cell. Signal. 40 (2017) 30–43, https://doi.org/10.1016/j.cellsig.2017.08.008.
[49] A. Singla, J. Wang, R. Yang, D.S. Geller, D.M. Loeb, B.H. Hoang, Wnt signaling in osteosarcoma, Curr. Adv. Sci. Osteosarcoma (2020) 125–139, https://doi.org/10.1007/978-3-030-43085-6_8.
[50] Y. Cai, A.B. Mohseny, M. Karperien, P.C. Hogendoorn, G. Zhou, A.-M. Cleton-Jansen, Inactive Wnt/β-catenin pathway in conventional high-grade osteosarcoma, J. Pathol. 220 (2010) 24–33, https://doi.org/10.1002/path.2628.
[51] T. Tanaka, T. Nakatani, T. Kamitani, Inhibition of NEDD8-conjugation pathway by novel molecules: potential approaches to anticancer therapy, Mol. Oncol. 6 (2012) 267–275, https://doi.org/10.1016/j.molonc.2012.01.003.
[52] X. Chen, Y. Wang, W. Zang, Y. Du, M. Li, G. Zhao, miR-194 targets RBX1 gene to modulate proliferation and migration of gastric cancer cells, Tumor Biol. 36 (2015) 2393–2401, https://doi.org/10.1007/s13277-014-2849-1.
[53] T. Kunishige, K. Migita, S. Matsumoto, K. Wakatsuki, H. Nakade, S. Miyao, H. Kuniyasu, M. Sho, Ring box protein-1 is associated with a poor prognosis and tumor progression in esophageal cancer, Oncol. Lett. 20 (2020) 2919–2927, https://doi.org/10.3892/ol.2020.11840.
[54] D.-J. Fu, T. Wang, Targeting NEDD8-activating enzyme for cancer therapy: developments, clinical trials, challenges and future research directions, J. Hematol. Oncol. 16 (2023) 87, https://doi.org/10.1186/s13045-023-01485-7.
[55] J. Xian, S. Wang, Y. Jiang, L. Li, L. Cai, P. Chen, Y. Liu, X. Zeng, G. Chen, C. Ding, R. M. Hoffman, L. Jia, H. Zhao, Y. Zhang, Overexpressed NEDD8 as a potential therapeutic target in esophageal squamous cell carcinoma, Cancer Biol. Med. 19 (2021) 504–517, https://doi.org/10.20892/j.issn.2095-3941.2020.0484.
[56] J. Shao, Q. Feng, W. Jiang, Y. Yang, Z. Liu, L. Li, W. Yang, Y. Zou, E3 ubiquitin ligase RBX1 drives the metastasis of triple negative breast cancer through a FBXO45-TWIST1-dependent degradation mechanism, Aging 14 (2022) 5493–5510, https://doi.org/10.18632/aging.204163.
[57] Y. Zhang, Y. Lei, J. Xu, J. Hua, B. Zhang, J. Liu, C. Liang, Q. Meng, X. Yu, S. Shi, Role of damage DNA-binding protein 1 in pancreatic cancer progression and chemoresistance, Cancers 11 (2019) 1998, https://doi.org/10.3390/cancers11121998.
[58] Fararjeh, Chen Ho, Cheng Liu, Chang Chang, Wu Tu, Proteasome 26S subunit, non-ATPase 3 (PSMD3) regulates breast cancer by stabilizing HER2 from degradation, Cancers 11 (2019) 527, https://doi.org/10.3390/cancers11040527.
[59] Y. Sun, Y. Sun, S. Yue, Y. Wang, F. Lu, Histone deacetylase inhibitors in cancer therapy, Curr. Top. Med. Chem. 18 (2019) 2420–2428, https://doi.org/10.2174/1568026619666181210152115.
[60] M. Rashid, L. Rostami, B. Baradaran, O. Molavi, Z. Ghesmati, M. Sabzichi, F. Ramezani, Up-down regulation of HIF-1 α in cancer progression 798 (2021).
[61] Y. Li, Y. Xu, R. Wang, W. Li, W. He, X. Luo, Y. Ye, Expression of Notch – Hif-1 a signaling pathway in liver regeneration of rats, (2020). https://doi.org/10.1177/0300060520943790.
[62] C.S. Nowell, F. Radtke, Notch as a tumour suppressor, Nat. Rev. Cancer 17 (2017) 145–159, https://doi.org/10.1038/nrc.2016.145.
[63] X. Li, Y. Cao, M. Li, F. Jin, Upregulation of HES1 promotes cell proliferation and invasion in breast cancer as a prognosis marker and therapy target via the AKT pathway and EMT process, J. Cancer 9 (2018) 757–766, https://doi.org/10.7150/jca.22319.
[64] I. Kulic, G. Robertson, L. Chang, J.H.E. Baker, W.W. Lockwood, W. Mok, M. Fuller, M. Fournier, N. Wong, V. Chou, M.D. Robinson, H. Chun, B. Gilks, B. Kempkes, T. A. Thomson, M. Hirst, A.I. Minchinton, W.L. Lam, S. Jones, M. Marra, A. Karsan, Loss of the notch effector RBPJ promotes tumorigenesis, J. Exp. Med. 212 (2015) 37–52, https://doi.org/10.1084/jem.20121192.
[65] T. Friedrich, F. Ferrante, L. Pioger, A. Nist, T. Stiewe, J. Andrau, M. Bartkuhn, B. D. Giaimo, T. Borggrefe, Notch-dependent and -independent functions of transcription factor RBPJ, Nucleic Acids Res. 50 (2022) 7925–7937, https://doi.org/10.1093/nar/gkac601.
[66] A. Caner, E. Asik, B. Ozpolat, SRC signaling in cancer and tumor microenvironment, : Tumor Micro. (2021) 57–71, https://doi.org/10.1007/978-3-030-47189-7_4.
[67] M. Asaduzzaman, S. Constantinou, H. Min, J. Gallon, M.L. Poonam, S. Selina, R. Simak, S. Shousha, R.C. Coombes, E.W. Lam, Y. Hu, E. Yagu, Tumour suppressor EP300, a modulator of paclitaxel resistance and stemness, is downregulated in metaplastic breast cancer, (2017) 461–474. https://doi.org/10.1007/s10549-017-4202-z.
[68] N. Attar, S.K. Kurdistani, Exploitation of EP300 and CREBBP lysine acetyltransferases by cancer, Cold Spring Harb. Perspect. Med. 7 (2017) a026534, https://doi.org/10.1101/cshperspect.a026534.
[69] S.R. Grossman, p300/CBP/p53 interaction and regulation of the p53 response, Eur. J. Biochem. 268 (2001) 2773–2778, https://doi.org/10.1046/j.1432-1327.2001.02226.x.
[70] H. Deng, L. Lv, Y. Li, C. Zhang, F. Meng, Y. Pu, J. Xiao, L. Qian, W. Zhao, Q. Liu, D. Zhang, Y. Wang, H. Zhang, Y. He, J. Zhu, The miR-193a-3p regulated PSEN1 gene suppresses the multi-chemoresistance of bladder cancer, Biochim. Biophys. Acta Mol. Basis Dis. 1852 (2015) 520–528, https://doi.org/10.1016/j.bbadis.2014.12.014.
[71] C. Feng, Y. Wang, Expression and Prognostic Analyses of ITGA3, ITGA5, and ITGA6 in Head and Neck Squamous Cell Carcinoma, (2020) 1–18. https://doi.org/10.12659/MSM.926800.
[72] L. Tian, M. Chen, Q. He, Q. Yan, C. Zhai, MicroRNA - 199a - 5p suppresses cell proliferation, migration and invasion by targeting ITGA3 in colorectal cancer, (2020) 2307–2317. https://doi.org/10.3892/mmr.2020.11323.
[73] Y. Deng, Q. Wan, W. Yan, Integrin α5/ITGA5 promotes the proliferation, migration, invasion and progression of oral squamous carcinoma By Epithelial–Mesenchymal transition, Cancer Manag. Res. 11 (2019) 9609–9620, https://doi.org/10.2147/CMAR.S223201.
[74] J. Xie, T. Guo, Z. Zhong, N. Wang, Y. Liang, W. Zeng, S. Liu, Q. Chen, X. Tang, H. Wu, S. Zhang, K. Ma, B. Wang, Y. Ou, W. Gu, H. Chen, Y. Qiu, Y. Duan, ITGB1 drives hepatocellular carcinoma progression by modulating cell cycle process through PXN/YWHAZ/AKT pathways, Front. Cell Dev. Biol. 9 (2021) 1–16, https://doi.org/10.3389/fcell.2021.711149.
[75] C. Song, V.J. Lowe, S. Lee, Inhibition of Cdc20 suppresses the metastasis in triple negative breast cancer (TNBC), Breast Cancer (2021), https://doi.org/10.1007/s12282-021-01242-z.
[76] Y. Shi, F. Yan, F. Wang, L. Pan, Tissue and Cell MiR-128-3p suppresses tumor proliferation and metastasis via targeting CDC6 in hepatocellular carcinoma cells, Tissue Cell 72 (2021) 101534, https://doi.org/10.1016/j.tice.2021.101534.
[77] D. Papini, M.D. Levasseur, J.M.G. Higgins, The aurora B gradient sustains kinetochore stability in anaphase, Cell Rep. 37 (2021) 109818, https://doi.org/10.1016/j.celrep.2021.109818.
[78] R. Schwarzer, H. Jiao, L. Wachsmuth, A. Tresch, R. Schwarzer, H. Jiao, L. Wachsmuth, A. Tresch, M. Pasparakis, FADD and Caspase-8 regulate gut homeostasis and inflammation by controlling MLKL- and GSDMD- mediated death of intestinal epithelial cells ll article FADD and Caspase-8 regulate gut homeostasis and inflammation by controlling MLKL- and GSDMD- mediated dea, Immunity 52 (2020) 978–993, https://doi.org/10.1016/j.immuni.2020.04.002.
[79] M.P. Amaral, K.R. Bortoluci, Caspase-8 and FADD: where cell death and inflammation collide, Immunity 52 (2020) 890–892, https://doi.org/10.1016/j.immuni.2020.05.008.
[80] V. Condelli, F. Crispo, M. Pietrafesa, G. Lettini, D.S. Matassa, F. Esposito, M. Landriscina, F. Maddalena, HSP90 molecular chaperones, metabolic rewiring, and epigenetics: impact on tumor progression and perspective for anticancer therapy, Cells 8 (2019) 532, https://doi.org/10.3390/cells8060532.
[81] K.-H. Song, S.J. Oh, S. Kim, H. Cho, H.-J. Lee, J.S. Song, J. Chung, E. Cho, J. Lee, S. Jeon, C. Yee, K. Lee, S.M. Hewitt, J.-H. Kim, S.R. Woo, T.W. Kim, HSP90A inhibition promotes anti-tumor immunity by reversing multi-modal resistance and stem-like property of immune-refractory tumors, Nat. Commun. 11 (2020) 562, https://doi.org/10.1038/s41467-019-14259-y.